Journal of Applied Polymer Science

Adsorption of Methylene Blue on Hemicellulose-Based Stimuli-Responsive Porous Hydrogel

Xiao-Feng Sun, Zhou Gan, Zhanxin Jing, Haihong Wang, Duo Wang, Yinan Jin
MOE Key Lab of Applied Physics and Chemistry in Space, Department of Applied Chemistry, College of Science, Northwestern Polytechnic University, Xi'an 710072, China
Correspondence to: X.-F. Sun (E-mail: xf001sn@nwpu.edu.cn)

ABSTRACT: A stimuli-responsive porous hydrogel was synthesized from wheat straw hemicellulose using $CaCO_3$ as the porogen, and its application for the removal of methylene blue was studied. The porous structure of the prepared hydrogel was confirmed by SEM analysis. The effects of pH and polyelectrolyte on the swelling of the hydrogels were discussed, and the porous hydrogels showed excellent sensitivity to pH and salt. The deswelling kinetic study indicated that the hydrogels exhibited rapid shrinking in NaCl aqueous solutions. The methylene blue adsorption on the hydrogels was investigated, and the obtained adsorption data was fitted to the pseudo-first-order, pseudo-second-order and intra-particle diffusion kinetics models, and the pseudo-first-order kinetic model could describe the adsorption process, and the adsorption process of methylene blue on the hydrogels was controlled by external film diffusion. This study reported that the hemicellulose-based porous hydrogel is promising for water treatment. © 2014 Wiley Periodicals, Inc. J. Appl. Polym. Sci. **2015**, *132*, 41606.

KEYWORDS: adsorption; biopolymers and renewable polymers; porous materials; swelling

Received 17 April 2014; accepted 7 October 2014
DOI: 10.1002/app.41606

INTRODUCTION

Superabsorbent hydrogels are three-dimensional network structural materials that can absorb and conserve considerable amounts of aqueous fluids,[1–3] and they are generally classified as conventional hydrogels and environmentally sensitive hydrogels because of their response to external stimuli. Environmentally sensitive hydrogels are also called intelligent hydrogels, and they can sense tiny environmental stimulus, such as temperature, electric fields, magnetic fields, light, pH, ionic strength, and pressure.[4] These hydrogels have been widely used in agriculture, environment, biomedicine, and other related fields, such as wastewater treatment,[5] drug delivery carriers,[6] artificial organs,[7] and tissue engineering.[8] In recent years, environmentally sensitive hydrogels have been widely used as adsorbents for the removal of hazardous substances from wastewater. Novel polyampholyte nanocomposite hydrogel had been synthesized, and the hydrogel was a suitable superabsorbent for removing indigo carmine from textile aqueous effluents.[9] Sema Ekici et al.[10] prepared poly (acrylamide-sepiolite) composite hydrogel, and the hydrogel was considered a candidate for retaining more water and dyes. The hydrogels based on the starch of potatoes had also been prepared, and these hydrogels had excellent adsorption capacities for cationic dye.[11]

Organic dyes are widely used in modern cosmetic, textiles, printing, and dyeing industries.[12] The colored wastewater from these industries is charged into the natural rivers, which results in a large area of water coloring that not only affects plant growth but also endangers human health. Dyes pollution can increase the chemical oxygen demand of water and decrease the projection of lighting which has an effect on photosynthesis.[13] The exposure to dye results in considerable damage, and a long-term exposure to dye can cause some side effects in the human body, such as a change in heart rate, vomiting, shock, limb paralysis, tissue death, and other adverse symptoms.[14,15] The removal of organic dye from wastewater had been studied using adsorption, biodegradation, oxidation, flocculation, and so on.[9] Adsorption is considered the most effective method for removing dye,[11] and the adsorbents based on natural polymers have attracted considerable attention for wastewater treatment applications because of their low-cost, biodegradation, and nontoxic behavior.

Hemicellulose (HC) is second only to cellulose as the most prevalent polysaccharide in nature, and it accounts for 30–40% of agriculture residues.[16] HC is heterogeneous polysaccharide consisting of various structural units,[17] and wheat straw HC is primarily composed of D-xylose, L-arabinose, D-mannose, D-glucose, D-glucuronic acid, and so on.[18] Because these structural units have an abundance of hydroxyl group, HC can be used to prepare hydrogels. A few functional hydrogels based on HC have been prepared,[19–22] and there is a currently promising research on preparing novel HC-based hydrogels for industrial applications.

Table I. Feed Compositions of the Porous HC-g-PSA Hydrogels

Sample code	AA (g)	HC (g)	AA/HC (g/g)	$CaCO_3$ (%)
Gel-1	2.0	0.5	4	20
Gel-2	3.0	0.5	6	20
Gel-3	4.0	0.5	8	20
Gel-4	5.0	0.5	10	20
Gel-5	6.0	0.5	12	20
Gel-6	4.0	0.5	8	0
Gel-7	4.0	0.5	8	5
Gel-8	4.0	0.5	8	10
Gel-9	4.0	0.5	8	15
Gel-10	4.0	0.5	8	30

$CaCO_3(\%) = \frac{CaCO_3}{HC+AA} \times 100\%$ (by weight).

The purpose of this study was to prepare HC-based porous hydrogels for removing methylene blue from aqueous solution. The prepared hydrogels were characterized using FT-IR and SEM. The pH- and salt-responses and the deswelling kinetics of the prepared hydrogels were investigated. The adsorption behavior of methylene blue onto the prepared hydrogels was also studied to test their potential for environmental applications.

EXPERIMENTAL

Materials

The monomer acrylic acid (AA) was purchased from the Tianjin Kermel Chemical Reagent Company in China. The cross-linker *N*,*N*′ methylenebisacrylamide (MBA), initiator ammonium persulfate (APS), and anhydrous sodium sulfite were purchased from the Tianjing Hongyan Chemical Reagent Factory in China. The porogen, $CaCO_3$, was purchased from the Tianjing Fuchen Chemical Reagent Factory in China. The methylene blue, which was used in the adsorption studies, was purchased from the Tianjing Tianli Chemical Reagent Factory in China. All other reagents were of analytical grade.

EXPERIMENTAL METHOD

Isolation and Characterization of HC from Wheat Straw

Wheat straw was first cut into small pieces and then dried in an oven at 60°C, and the dried materials were dewaxed using toluene and ethanol in a 2 : 1 volume ratio in a Soxhlet apparatus for 12 h. The dewaxed straw was delignified using sodium chlorite in an acidic solution (pH 4.0) at 75°C for 2 h to obtain holocellulose. The holocellulose was treated using 10% KOH at a 1 : 20 solid to liquid ratio at room temperature for 10 h and then filtered to separate HC and cellulose. The obtained filtrate was neutralized to pH 5.5 and concentrated under a reduced pressure, and then precipitated in three volumes of ethanol to obtain HC materials.

The prepared HC contained 80.4% xylose and 12.5% arabinose (related to the total sugar content), which was determined using our previous method by gas chromatography.[16] The values of the weight-average and number-average molecular weights of the HC were 28,650 and 13,770 g mol^{-1}, respectively, which were determined using GPC.

Synthesis of Porous Hemicellulose-*g*-poly(sodium acrylate) Hydrogels

Hemicellulose-*g*-poly(sodium acrylate) porous hydrogels (HC-*g*-PSA) were prepared by free radical polymerization method. About 0.5 g of HC was dissolved into a 10 mL solution of 6% NaOH (wt %), and a certain amount of $CaCO_3$ particles with 120-nm diameter was added into the HC solution. Then, 0.05 g of both the APS initiator and the anhydrous sodium sulfite accelerant were added into the mixed solution, and the sodium acrylate solution and 0.05 g of the MBA cross-linker were also added into the solution. The sodium acrylate solution was prepared by dissolving the appropriate amount of AA into 10 mL of distilled water and then neutralized with NaOH. When the viscosity of the reaction mixture increased, the stirring was stopped. The reaction beaker was placed in a water bath at 25°C for 1 h to ensure a complete reaction. The prepared hydrogels were collected and cut into uniform sized pieces, and these pieces were immersed into 0.1 mol L^{-1} HCl solutions to remove $CaCO_3$, and the HCl solution was replaced regularly until there were no bubbles on the surface of the hydrogels and the hydrogels floated on the surface of the solution. Hydrogels free of $CaCO_3$ were then immersed into dilute alkali solution to convert —COOH into —COO^- completely. The prepared HC-*g*-PSA hydrogel samples were placed into an oven and dried until a constant weight was obtained. The feed compositions for the preparations of HC-*g*-PSA hydrogels are presented in Table I.

Hydrogel Characterization

The chemical structure of the prepared hydrogels were analyzed using Fourier transform infrared spectrophotometer (Nicolet 510) within a frequency range of 4000–400 cm^{-1} after the samples were mixed with KBr and pressed to form a disc. The surface morphology of the prepared hydrogels were observed using a scanning electron microscope (SEM, S-2460N, Hitachi, Tokyo, Japan) after the swollen hydrogel samples were freeze-dried and coated with gold.

Swelling Test

The swelling ratio of the hydrogel samples was determined using gravimetric method in buffer solutions with different pH (2.0–12.0) and in NaCl or $CaCl_2$ solutions with various concentrations (0.01–0.10 mol L^{-1}) at room temperature. The ionic strengths of all of the buffer solutions were adjusted to 0.05 *M* using NaCl. To ensure complete swelling, samples were allowed to swell for 2 days, and the swollen hydrogel samples were then weighed after the excess surface water was removed using filter papers. The equilibrium swelling ratio (SR) was calculated using the following eq. (1):

$$\text{SR (g/g)} = \frac{W_e - W_d}{W_d} \quad (1)$$

where W_e is the weight of the swollen hydrogel (g) and W_d is the weight of the dry hydrogel (g).

The shrinking rate of hydrogels is very important for their potential applications. The deswelling kinetics of hydrogels is generally studied in salt solutions, and the water retention values are used to evaluate the deswelling kinetics. During this test, swollen hydrogel samples were immersed into a

0.05 mol L^{-1} NaCl solution at room temperature. After certain time intervals, the samples were collected and weighed after removing the excess water from the surface of the hydrogel. The water retention (WR) was calculated using the following eq. (2):

$$\mathrm{WR}\,(\%) = \frac{W_t - W_d}{W_e - W_d} \times 100\% \quad (2)$$

where W_t is the weight of the hydrogel (g) at deswelling time t (min), and W_d is the weight of the dry hydrogel (g), and W_e is the weight of the swollen hydrogel (g).

Adsorption and Desorption Test

The adsorption property of the prepared hydrogels for cationic dye removal was studied using methylene blue as a model compound. Approximately 20 mg of dried hydrogel was immersed in 50 mL solutions of methylene blue for 72 h at room temperature, and the concentrations of the methylene blue solutions before and after adsorption were then measured using a UV spectrophotometer at 663 nm.[23] The effect of temperature on adsorption and desorption behavior was studied at the temperatures of 30, 40, 50, 60, and 70°C. Desorption test was performed in distilled water using the hydrogel sample containing methylene blue.

The adsorption amount of methylene blue (Q) was determined using the eq. (3):

$$Q(\mathrm{mg/g}) = \frac{(C_o - C_e) \times V}{1000\, W_d} \quad (3)$$

The removal/desorption percentage of methylene blue was calculated using eq. (4):

$$R(\%) = \frac{C_o - C_e}{C_o} \times 100\% \quad (4)$$

where C_o and C_e are the initial concentration and the remaining concentration of the used solution (mg L^{-1}), respectively; V is the volume of the used solution (mL), and W_d is the weight of the dried hydrogel (g).

RESULTS AND DISCUSSION

Preparation of Porous HC-*g*-PSA Hydrogels

The proposed mechanism for the synthesis of porous HC-*g*-PSA is shown in Figure 1. First, the redox initiator system $(NH_4)_2S_2O_8$-$NaSO_3$ deprived of hydrogen from the HC hydroxyl group. The grafting reaction occurred at the active sites of the hemicellulosic polymers by sodium acrylate. The two end vinyl groups of the MBA cross-linker could react with some active sites to form a polymeric network. During the preparation process, $CaCO_3$ was added as a porogen, and the hydrogels containing $CaCO_3$ were obtained; $CaCO_3$ was then removed by washing the hydrogels with a diluted acid. The obtained hydrogel samples were treated with a NaOH solution to convert the —COOH groups into —COO— groups completely.

FT-IR Analysis of HC-*g*-PSA Hydrogels

Figure 2 presents the FT-IR spectra of HC, Gel-3, and Gel-4. The IR spectrum of HC presented the absorption peaks at 3442, 2923, 1630, 1467, 1256, 1044, and 901 cm^{-1}, which are the characteristic absorptions of hemicellulosic polymer.[16] The

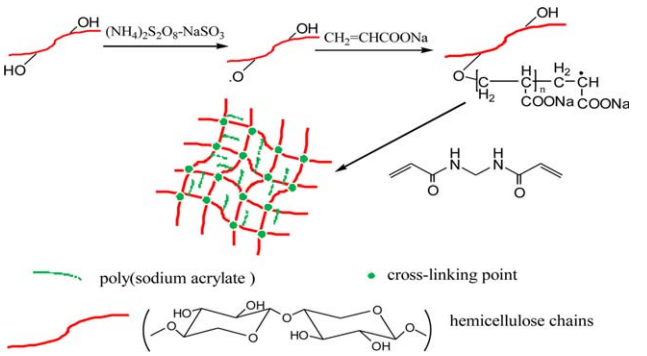

Figure 1. Proposed mechanism for the synthesis of the porous HC-*g*-PSA hydrogels. [Color figure can be viewed in the online issue, which is available at wileyonlinelibrary.com.]

absorption peak at 3442 cm^{-1} was assigned to the stretching of the O—H groups, and the band at 2923 cm^{-1} was attributed to the stretching of the C—H of methyl and methylene groups. The band at 1630 cm^{-1} can be assigned to the —OH bending from the absorbed water. The very small band at 1467 cm^{-1} was indicative of a trace amount of lignin in the HC. The sharp peak at 901 cm^{-1} was the frequency vibration and the ring frequency vibration of the C1 group, which is the characteristic absorption peak of the β-glycosidic bond. The band at 1044 cm^{-1} was attributed to the C—O and C—C stretching and the glycosidic linkage ν(C—O—C) contributions, which is the characteristic peak of xylan,[17] and indicated that the HC of wheat straw mainly consisted of xylan.

The IR spectra of HC-*g*-PSA hydrogel samples (Gel-3 and Gel-4) also exhibited the characteristic absorption peak of xylan at 1044 cm^{-1}, but the peak was relatively smaller than that in HC, which was due to the low content of added HC in the hydrogel. The spectra of hydrogels, except for the characteristic peaks of HC, presented two peaks at 1598 and 1401 cm^{-1}, which were assigned to the asymmetric and symmetric stretching of C=O in $-COO^-$ groups.[11] This observation indicated that sodium acrylate was successfully grafted to the HC.

SEM Analysis

SEM micrographs of the prepared hydrogels are also presented in Figure 3. As shown, the surface of the hydrogels that prepared without $CaCO_3$ was relatively slick, but the other hydrogels exhibited a large number of pores, and the pore distribution was well proportioned. Moreover, the content of the interconnected pore channels increased with increasing amounts of $CaCO_3$. The porous hydrogels that prepared using the porogen method mainly took the advantage of memory effect of the hydrogel, and the produced pores would not vanish after the removal of the porogen.[24]

Swelling Studies

Effects of pH on Swelling Behavior. The HC-*g*-PSA hydrogels would be sensitive to pH because of the presence of carboxylate groups in the hydrogels. The effect of pH on the equilibrium swelling ratio of the hydrogels is shown in Figure 4(a,b). As shown, the swelling ratio of all hydrogels in buffer solutions were low and significantly changed with increasing pH values of the buffer solution. Under strongly acidic conditions, the

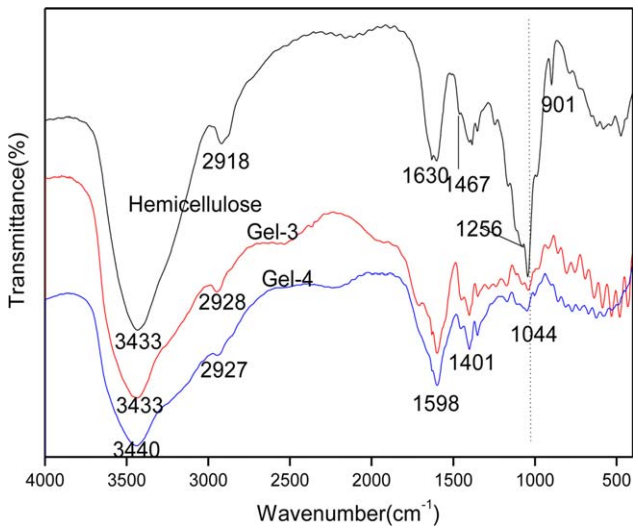

Figure 2. FT-IR spectra of the prepared hydrogels and HC. [Color figure can be viewed in the online issue, which is available at wileyonlinelibrary.com.]

swelling property of the prepared hydrogels was poor and the swelling ratio of the samples were <40 g g^{-1}, because the $-COO^-$ in the hydrogels was protonated which increased the number of hydrogen bonds in the hydrogel network and reduced the repulsive force. It is known that the dissociation constant, pK_a, of the carboxyl group is 4.28, and the carboxyl group would dissociate to $-COO^-$ when $pH > pK_a$, and this dissociation would result in a decreased number of hydrogen bonds and increase the repulsive forces among the negatively charged polymer chains; therefore, the equilibrium swelling ratio of hydrogel increased at $pH > 4$. At $pH > 8$, the $-COOH$ was completely ionized and the electrostatic repulsion force in the hydrogel network did not increase; therefore, the swelling ratio reached the maximum value and did not change with further increasing pH values.

Figure 4(a) displays the effect of the AA/HC ratio on the equilibrium swelling ratio of the prepared hydrogels, and the swelling ratio clearly decreased as the AA/HC ratio increased. The reason for this behavior is that the high AA content may result in more hydrogen bonds and restrict the movement of the molecular chains, which resulted in a denser network structure with smaller pores or space for water storage.[22] Figure 4(b) shows the effect of $CaCO_3$ amount on the equilibrium swelling ratio of the prepared hydrogel, and the swelling ratio of all samples was observed to increase with increasing the amount of $CaCO_3$. The addition of $CaCO_3$ nanoparticles resulted in high pore density which provided more paths for water molecule to

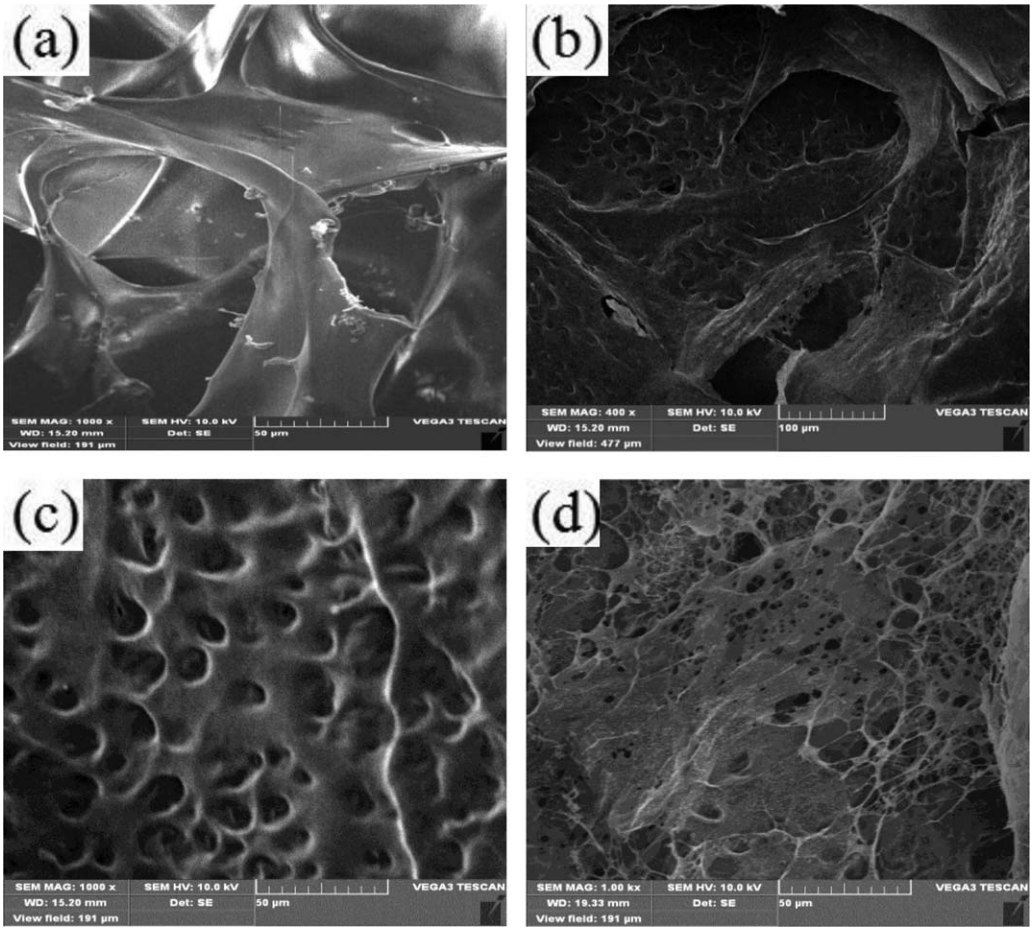

Figure 3. SEM images of the prepared porous hydrogel samples (a: Gel-6 ×400; b: Gel-3 ×400; c: Gel-3 ×1000; d: Gel-10 ×1000).

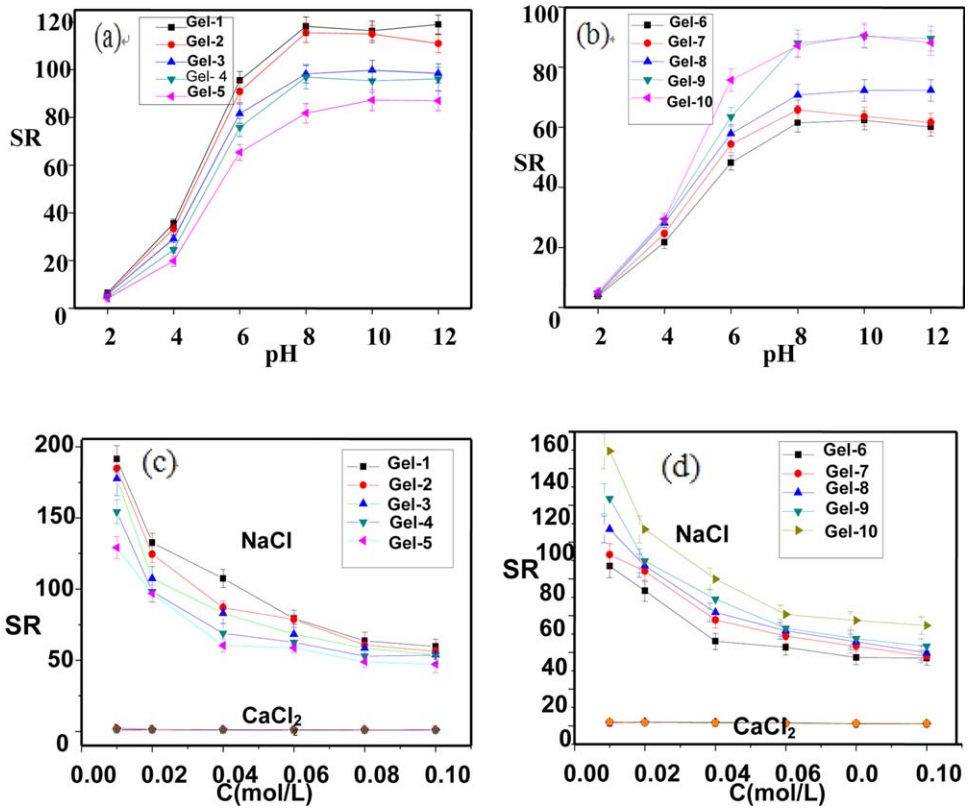

Figure 4. The change of the swelling ratio of the porous hydrogels: (a) hydrogels with various AA/HC ratios at different pH; (b) hydrogels with various amounts of $CaCO_3$ at different pH; (c) hydrogels with various AA/HC ratios in NaCl and $CaCl_2$ solutions; (d) hydrogels with various amounts of $CaCO_3$ in NaCl and $CaCl_2$ solutions. [Color figure can be viewed in the online issue, which is available at wileyonlinelibrary.com.]

diffuse into the hydrogel network.[25] Figure 5(a) presents the effect of temperature on the equilibrium swelling ratio of the prepared hydrogel, and it was observed that the swelling ratio significantly increased with an increase in temperature from 30 to 70°C, and this phenomenon implied that the high temperature promoted the swelling behavior of the hydrogel. The swelling process of hydrogel is generally controlled by three consecutive steps: the diffusion of water molecule into the polymer system, the relaxation of the hydrated polymer chains and expansion of the polymer network into the aqueous solution, which could be favored at higher temperature, and the pore size within the network could be increased at higher temperature.

Effect of Polyelectrolyte on Swelling Behavior. The prepared hydrogels in this study contained ionic carboxylate groups. According to the reports of Chang et al.[2] and Rasool et al.,[26] the effect of salt ions on the swelling of ionized hydrogels was remarkable. Therefore, the change in the swelling ratio of the hydrogel versus salt concentration and salt species was investigated, and the acquired results are displayed in Figure 4(c,d). The equilibrium swelling ratios of the prepared hydrogels were observed to decrease rapidly as the salt concentration increased, and this may result from the charge screening effect that caused by cationic Na^+ and Ca^{2+} which reduced the electrostatic repulsion force between carboxylate anions[1,2] and the osmotic pressure between the hydrogel network and the external solution. However, the decrease extent of the osmotic pressure was significant with an increasing salt concentration; therefore, the swelling ratios of the hydrogels rapidly reduced. Moreover, the swelling ratio of the hydrogel was significantly lower in the $CaCl_2$ solution than that in the NaCl solution, and this result indicated that Ca^{2+} ions may cross-link to polyacrylate, and the result was attributed to the difference in their charge number ($Ca^{2+} > Na^+$) which resulted in an ionic strength difference.[26] Therefore, the sensitivity of the hydrogel was greater in $CaCl_2$ solution than that in NaCl solution when their concentrations were kept the same.

Deswelling Kinetics. Deswelling behavior is a feature of ionized hydrogels, and deswelling study is significant for the application of the hydrogel in water treatment. Figure 6 presents the deswelling kinetics of the swollen hydrogel samples in a 0.05 mol L^{-1} NaCl solution at room temperature. As shown, the hydrogels rapidly shrunk and lost water once the swollen hydrogels were immersed into the NaCl solution. The hydrogels could reach the shrinking equilibrium after ~200 min. The effect of AA/HC ratio on the deswelling kinetics is presented in Figure 6(a), and the water retention value increased from 15.60 to 24.16% when the AA/HC ratio increased from 4 to 12; therefore, the shrinking rate clearly decreased as the AA/HC ratio increased. The shrinking of hydrogels primarily depended on the charge screening effect that caused by the cationic Na^+, which resulted in a decrease of the electrostatic repulsion force between carboxylate anions.[2,26] When the AA/HC ratio was

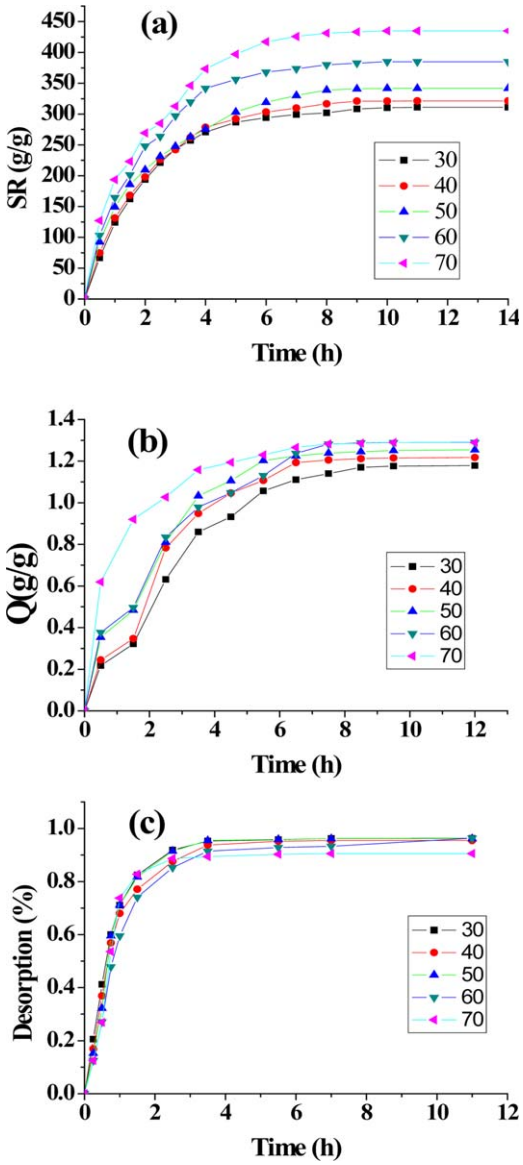

Figure 5. Effect of temperature on the swelling ratio (a), adsorption (b) and desorption (c) of the prepared hydrogel. [Color figure can be viewed in the online issue, which is available at wileyonlinelibrary.com.]

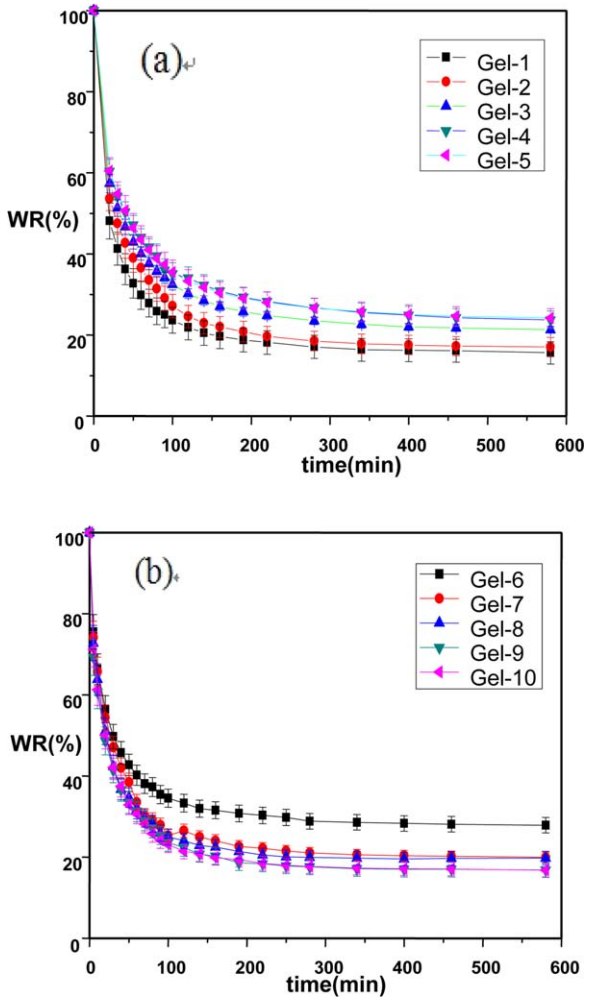

Figure 6. Deswelling kinetics of the porous hydrogels in a 0.05 mol L^{-1} NaCl solution: (a) hydrogels with various AA/HC ratios; (b) hydrogels with various amounts of $CaCO_3$. [Color figure can be viewed in the online issue, which is available at wileyonlinelibrary.com.]

high, the charge screening effect was reduced. Figure 6(b) presents the effect of $CaCO_3$ amount on the deswelling kinetics, and the water retention value decreased from 27.88 to 16.78% when the amount of $CaCO_3$ was increased from 0 to 30%. Because of the increased number of pores with the increasing amount of $CaCO_3$, the water molecules in the hydrogel network can be excluded. The pores offered excluded paths for water molecule diffusion from the hydrogel network.[25]

Adsorption Studies

Effect of Initial Concentration of Methylene Blue on Adsorption. Figure 7(a) shows that the adsorption amount of methylene blue was dependent on initial concentrations. The adsorption amount of methylene blue on the porous HC-*g*-PSA hydrogel clearly increased from 58.7 to 1072.7 mg g^{-1} as the initial concentration increased from 25 to 500 mg L^{-1}, respectively. This result may be due to the more concentrated solution inducing a stronger driving force.[27] Rafatullah et al.[28] had reviewed the adsorption of methylene on low-cost adsorbents, and Yagub et al.[29] had reviewed dye removal from aqueous solution by adsorption, and the adsorption capacity of the listed adsorbents was less than 1000 mg g^{-1}, and the prepared hydrogel showed higher adsorption amount of methylene blue. The removal percentage of methylene blue by the prepared hydrogel was >87% when the initial concentration of methylene blue was <300 mg L^{-1}, and it decreased with increasing initial concentration because of the use of only 20 mg hydrogel samples. We prepared hemicellulose-*g*-poly(methacrylic acid)/carbon nanotube composite hydrogel for methylene bule removal,[30] and the removal percentage was kept higher than 98% when the adsorbent amount was above 6 g L^{-1}, but the adsorption capacity of methylene blue was very low.

The SEM images of Gel-10 before and after adsorbing methylene blue are presented in Figure 8(a,b), respectively. Figure 8(b) shows that the pore structure of the hydrogel sample with methylene blue had not been observed, which was attributed to

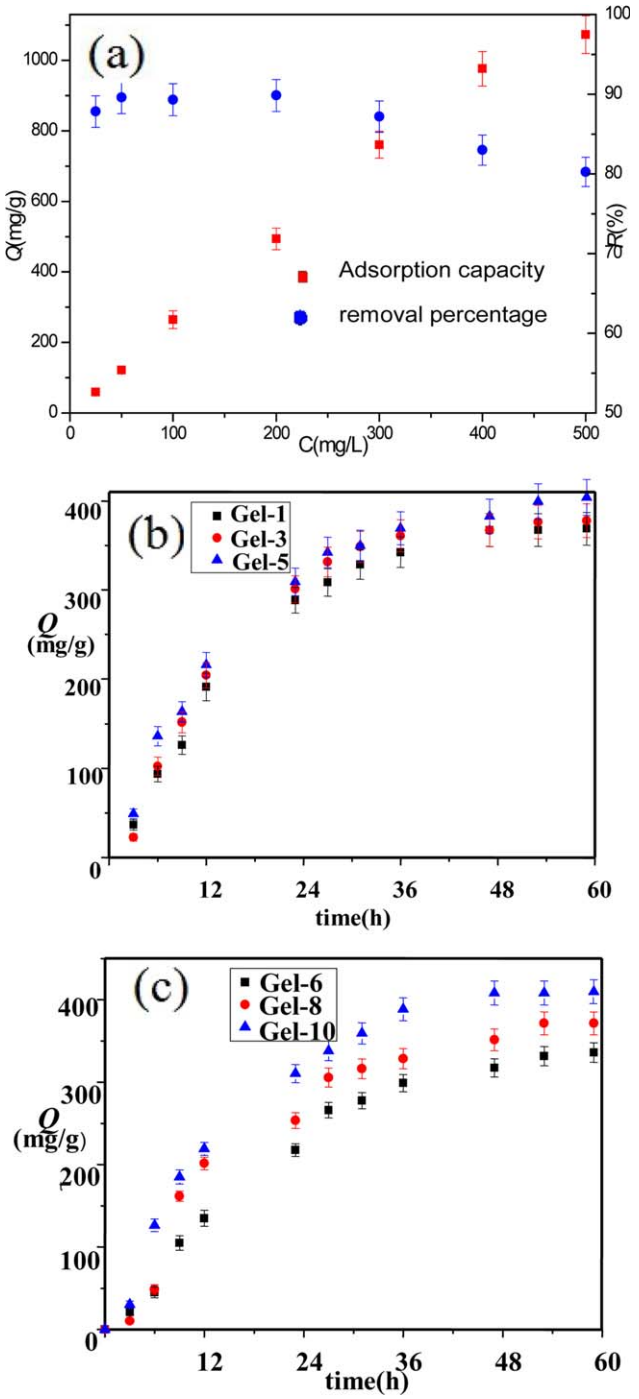

Figure 7. Effects of the initial concentration and contact time on the adsorption: (a) Effect of initial concentration; (b) Effect of contact time on the hydrogels with various AA/HC ratios; (c) Effect of contact time on the hydrogels with various amounts of $CaCO_3$. [Color figure can be viewed in the online issue, which is available at wileyonlinelibrary.com.]

the reduction in the repulsive force between the polymer chains after the adsorption of the cationic dye on anionic hydrogel, thereby causing a decrease in the pore size. Because methylene blue is a cationic dye and the surface of HC-*g*-PSA hydrogels contained a large number of —COO^- groups, the strong electrostatic attraction resulted in the high removal percentage. In a previous paper,[30] we had studied the FT-IR spectra of methylene blue loaded sample, and found that the adsorption of methylene blue on the hydrogel mainly depended on electrostatic interactions between —COO^- anions and methylene blue molecules.

Effect of Contact Time on Adsorption. Figure 7(b,c) presents the plots for the amount of adsorbed methylene blue vs. contact time at an initial concentration of 200 mg L^{-1}. The amount of adsorbed dye was observed to increase as the contact time increased, and the uptake of methylene blue was rapid during the initial 36-h period, and the adsorption quantity achieved >90% of the equilibrium adsorption amount. After 59 h, all of the hydrogel samples accomplished adsorption equilibrium. Figure 7(b) presents the effect of the AA/HC ratio on the adsorption amount, and there was no evident difference in the adsorption capacity of the porous hydrogels prepared with varied AA/HC ratios. The adsorption capacity may be affected by both the swelling ratio of the hydrogels and the amount of —COO^- groups, and the swelling ratio data of samples indicated Gel-1>Gel-3>Gel-5 but the amount of —COO^- groups in hydrogels was Gel-1<Gel-3<Gel-5; therefore, the effect of the AA/HC ratio on the adsorption capacity may be not significant. The adsorption capacity of the porous HC-*g*-PSA hydrogels that were synthesized with various amounts of $CaCO_3$ is displayed in Figure 7(c). The adsorption amount clearly improved as the used $CaCO_3$ amount increased, and this improvement is because the addition of $CaCO_3$ increased the number of pores in the hydrogel, which not only created a chance for adsorbing methylene blue but also resulted in complete exposure of the —COO^- in the hydrogel. Therefore, the adsorption amount of methylene blue on the porous HC-*g*-PSA hydrogel increased with the addition of $CaCO_3$ nanoparticles.

Effect of Temperature on Adsorption and Desorption. Temperature may affect the adsorption and desorption behaviors. Figure 5(b,c) presents the effect of temperature on the adsorption amount and desorption percentage of methylene blue on the prepared hydrogel, respectively. As shown, temperature affected the adsorption behavior of the prepared hydrogel, and the adsorption amount of methylene blue was 1280 mg g^{-1} at 70°C that was higher than that at 30°C (1180 mg g^{-1}), and the adsorption behavior was fast during the initial 4 h at 70°C, indicating an endothermic process; However, temperature did not significantly affect the desorption behavior of methylene blue on the prepared hydrogel, and the desorption percentage of methylene blue reached 96% at 30°C. This result indicated that the prepared hydrogel can be reused for methylene blue removal and an increase of temperature can promote the adsorption behavior but not affect the desorption behavior of methylene blue on the prepared hydrogel.

Adsorption Kinetics. To clarify the adsorption process of methylene blue on the porous HC-*g*-PSA hydrogel, the adsorption kinetics was studied. The obtained experimental data were fitted using the pseudo-first-order kinetics model and the pseudo-second-order kinetics model. A linear form of the pseudo-first-order kinetics model is expressed by the following eq. (5)[31,32]:

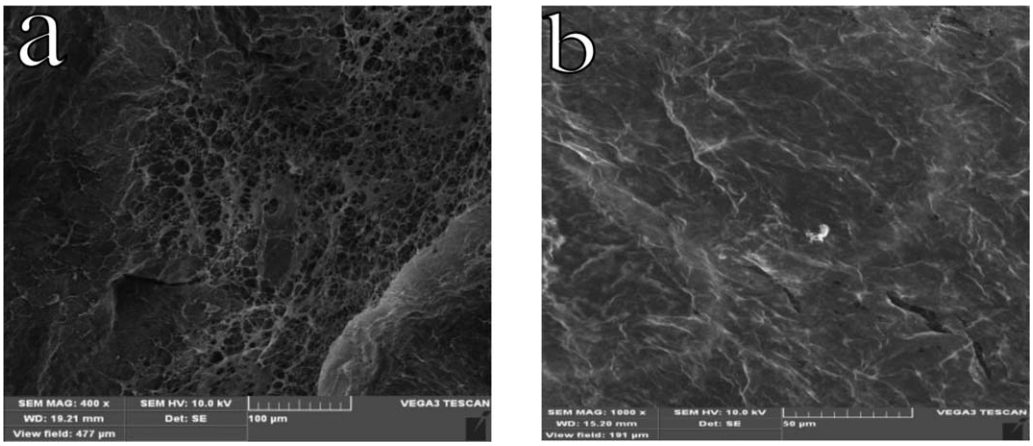

Figure 8. SEM images of Gel-10 before adsorbing methylene blue (a) and after adsorbing methylene blue (b).

$$\log(Q_e - Q_t) = \log Q_e - \frac{k_1 t}{2.303} \quad (5)$$

A linear form of the pseudo-second-order kinetics model is expressed by the following eq. (6)[33,34]

$$\frac{t}{Q_t} = \frac{1}{k_2 Q_e^2} + \frac{t}{Q_e} \quad (6)$$

where Q_t is the amount of methylene blue adsorbed at time t and Q_e is the amount at equilibrium state (mg g^{-1}); k_1 (h^{-1}) and k_2 (g mg^{-1} h^{-1}) are the rate constants of the pseudo-first-order kinetics model and the pseudo-second-order kinetics model, respectively.

The fitting results from the pseudo-first-order kinetics model and the pseudo-second-order kinetics model are listed in Table II. The R^2 values for the pseudo-first-order kinetics model were >0.94, whereas the R^2 values for the pseudo-second-order kinetics model were lower for all samples, which indicated that the pseudo-first-order kinetic model was appropriate for predicating the kinetics of methylene blue adsorption on the porous hydrogels. This result suggested that the adsorption of methylene blue on the hydrogels was a chemsorption process that involved the exchange or sharing of electrons between methylene blue and the functional groups on the HC-*g*-PSA hydrogels. Table II shows that the experimentally determined adsorption capacity was less than that determined by calculation. This may be due to the change of porous structure of the hydrogel during the adsorption process. The methylene blue adsorption on the porous HC-*g*-PSA hydrogels primarily depended on the electrostatic attraction between methylene blue and the functional groups on the hydrogel, which reduced the repulsive forces in the hydrogel network. As shown from Figure 8(b), the pores on the surface of the hydrogel could be not observed, and this result is due to the reduction in the repulsive forces that limited the diffusion of the methylene blue molecule into the inside of the adsorbent, thereby causing the decreases in the experimental adsorption amount of methylene blue.

Table II. Adsorption Kinetic Parameters of Methylene Blue onto Porous Hydrogels

Sample code	Gel-1	Gel-3	Gel-5	Gel-6	Gel-8	Gel-10
Q_e[a], mg g^{-1}	368.80	377.86	403.89	298.96	350.09	409.86
Pseudo-first-order						
K_1, h^{-1}	0.0990	0.0921	0.0737	0.0612	0.0636	0.0753
Q_e[b], mg g^{-1}	573.72	501.53	459.41	384.45	408.75	461.35
R^2	0.9455	0.9565	0.9584	0.9863	0.9852	0.9665
Pseudo-second-order						
K_2, g mg^{-1} h × 10^{-5}	4.7043	0.5569	7.6919	0.9319	0.0016	4.0490
Q_e[b], mg g^{-1}	628.93	1434.50	578.03	1045.09	−21845.32	709.22
R^2	0.8797	−0.0352	0.9561	0.3312	−0.1109	0.6946
Intra-particle diffusion						
k_{id}, mg g^{-1} $h^{1/2}$	68.7461	70.9761	67.2414	63.9045	68.8204	72.9716
C_i	−66.9188	−64.6804	−34.2675	−90.2436	−78.9007	−53.7708
R^2	0.9673	0.9420	0.9540	0.9757	0.9248	0.9619

[a] Experimental.
[b] Calculated.

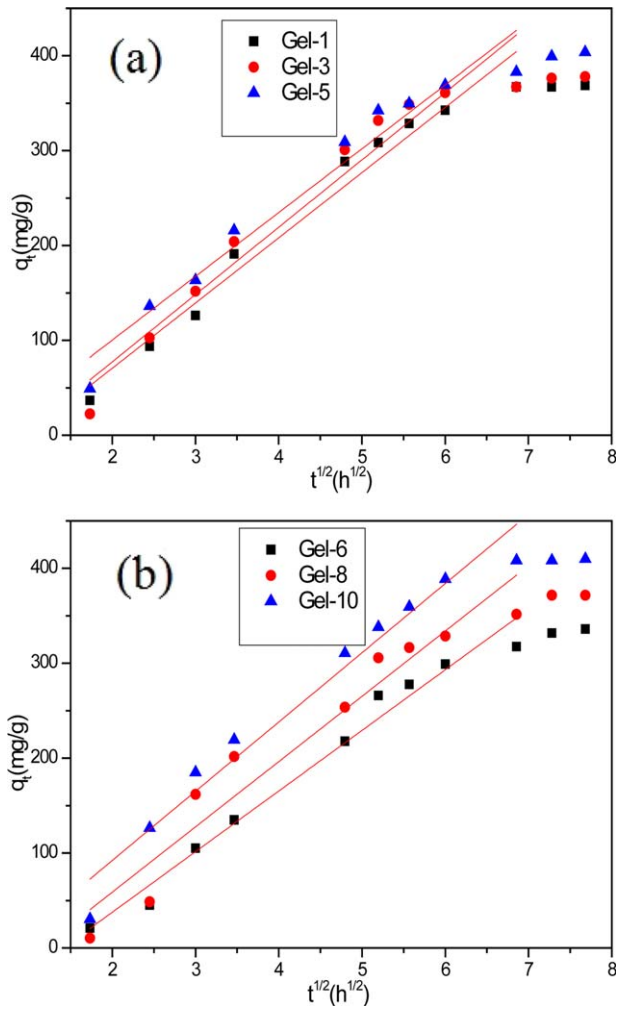

Figure 9. Intraparticle diffusion plots for methylene blue adsorption into the porous hydrogels: (a) hydrogels with various AA/HC ratios; (b) hydrogels with various amounts of $CaCO_3$. [Color figure can be viewed in the online issue, which is available at wileyonlinelibrary.com.]

To study the adsorption mechanism of methylene blue on the porous HC-*g*-PSA hydrogels, the experimental data were also fitted using the intra-particle diffusion kinetics model. This model is expressed by the eq. (7)[35,36]:

$$Q_t = k_{id} t^{1/2} + C_i \quad (7)$$

where k_{id} (mg/g $h^{1/2}$) is the diffusion rate of the intra-particle diffusion kinetics model; t (h) represents time; C_i is a constant.

If the plot of Q_t vs. $t^{1/2}$ passes through the origin, the intra-particle diffusion is the rate-limiting step. If C_i is not zero, the adsorption process may be controlled by both external film and intra-particle diffusion. When the plots exhibit multilinearity, it indicates that many steps occur during the adsorption process.[37]

Figure 9 presents the plot of Q_t vs. $t^{1/2}$ for the methylene blue adsorption on the porous HC-*g*-PSA hydrogels. The values of k_{id} and C_i are also listed in Table II. Figure 9 shows that the experimental data points before 36 h almost formed a straight line and did not pass through origin, which indicated that the external film diffusion occurred during the adsorption process, and this stage was likely due to the strong electrostatic attraction between methylene blue and the external surface of the adsorbent. After 36 h, adsorption behavior was attributed to the diffusion of methylene blue molecules to inside the porous HC-*g*-PSA hydrogels through pores. However, the pore shrinking of the adsorbent limited the diffusion of dye molecules to inside the adsorbent.

CONCLUSIONS

A novel porous hydrogel based on HC was synthesized using $CaCO_3$ as the porogen. The porous HC-*g*-PSA hydrogel showed a high adsorption capacity for methylene blue. The effect of the AA/HC ratio on the adsorption capacity was not significant, and the adsorption capacity improved with an increasing amount of used $CaCO_3$. The study of the adsorption kinetics demonstrated that the pseudo-first-order kinetics model was suitable for describing the adsorption process of methylene blue on the porous HC-*g*-PSA hydrogels. The smart swelling property and the high adsorption capacity of the porous HC-*g*-PSA hydrogels will be very significant for wastewater treatment application.

ACKNOWLEDGMENTS

The authors thank for jointly supporting by Graduate Starting Seed Fund and Foundation for Fundamental Research of Northwestern Polytechnical University (No. Z2014072 and NPU-FFR-JC20110274).

REFERENCES

1. Chang, C. Y.; Duan, B.; Cai, J.; Zhang, L. N. *Eur. Polym. J.* **2010**, *46*, 92.
2. Chang, C.; He, M.; Zhou, J.; Zhang, L. *Macromolecules* **2011**, *46*, 1642.
3. Wang, W. B.; Wang, A. Q. *Carbohydr. Polym.* **2010**, *80*, 1028.
4. Dumitriu, R. P.; Mitchell, G. R.; Vasile, C. *Polym. Int.* **2011**, *60*, 222.
5. Shen, C.; Shen, Y.; Wen, Y.; Wang, H.; Liu, W. *Water Res.* **2011**, *45*, 5200.
6. Mandal, B. B.; Kapoor, S.; Kundu, S. C. *Biomaterials* **2009**, *30*, 2826.
7. Eyholzer, C.; Borges, de Couraca, A.; Duc, F.; Bourban, P. E.; Tingaut, P.; Zimmermann, T.; Manson, J. A. E.; Oksman, K. *Biomacromolecules* **2011**, *12*, 1419.
8. Yang, M. J.; Chen, C. H.; Lin, P. J.; Huang, C. H.; Chen, W.; Sung, H. S. *Biomacromolecules* **2007**, *8*, 2746.
9. Dalaran, M.; Emik, S.; Güçlü, G.; İyim, T. B.; Özgümüs, S. *Desalination* **2011**, *279*, 170.
10. Ekici, S.; Isikver, Y.; Saraydin, D. *Polym. Bull.* **2006**, *57*, 231.
11. Dragan, E. S.; Apopei, D. F. *Chem. Eng. J.* **2011**, *178*, 252.
12. Jeon, Y. S.; Lei, J.; Kim, J. H. *J. Ind. Eng. Chem.* **2008**, *14*, 726.
13. Bulut, Y.; Aydin, H. *Desalination* **2006**, *194*, 259.
14. Yi, J. Z.; Zhang, L. M. *Bioresource Technol.* **2008**, *99*, 2182.

15. Rubín, E.; Rodríguez, P.; Herrero, R.; Sastre,; de Vicente, M. E. *J. Chem. Eng. Data* **2010**, *55*, 5707.
16. Sun, X. F.; Jing, Z. X.; Fowler, P.; Wu, Y. G.; Rajaratnam, M. *Ind. Crop Prod.* **2011**, *33*, 588.
17. Sun, X. F.; Sun, R. C.; Fowler, P.; Baird, M. S. *J. Agr. Food Chem.* **2005**, *53*, 860.
18. Lawther, J. M.; Sun, R. C.; Banks, W. B. *J. Agric. Food Chem.* **1995**, *43*, 667.
19. Gröndahl, M.; Eriksson, L.; Gatenholm, P. *Biomacromolecules* **2004**, *5*, 1528.
20. Lindblad, M. S.; Albertsson, A. C.; Ranucci, E.; Laus, M.; Giani, E. *Biomacromolecules* **2005**, *6*, 684.
21. Hettrich, K.; Fanter, C. *Macromol. Symp.* **2010**, *294*, 141.
22. Sun, X. F.; Wang, H. H.; Jing, Z. X.; Rajaratnam, M. *Carbohydr. Polym.* **2013**, *92*, 1357.
23. Dogan, M.; Alkan, M.; Türkyilmaz, A.; Özdemir, Y. *J. Hazard. Mater.* **2004**, *109*, 141.
24. Lu, G.; Yan, Q.; Su, X.; Liu, Z.; Ge, C. *Prog. Chem.* **2007**, *19*, 485.
25. Liu, X. H.; Wang, X. G.; Liu, D. S. *Acta. Polym. Sin.* **2002**, *3*, 354.
26. Rasool, N.; Yasin, T.; Heng, J. Y. Y.; Akhter, Z. *Polymer* **2010**, *51*, 1687.
27. Solpana, D.; Duran, S.; Saraydin, D.; Guven, O. *Radiat. Phys. Chem.* **2003**, *66*, 117.
28. Rafatullah, M.; Sulaiman, O.; Hashim, R.; Ahmad, A. *J. Hazard. Mater.* **2010**, *177*, 70.
29. Yagub, M. T.; Sen, T. K.; Afroze, S.; Ang, H. M. *Adv. Colloid Interfac.* **2014**, *209*, 172.
30. Sun, X. F.; Ye, Q.; Jing, Z. X.; Li, Y. *J. Polym. Compos.* **2014**, *35*, 45.
31. Wang, S.; Li, H. *Dyes & Pigments* **2007**, *72*, 308.
32. Dulman, V.; Simion, C.; Bârsănescu, A.; Bunia, I.; Neagu, V. *J. Appl. Polym. Sci.* **2009**, *113*, 615.
33. Loukidou, M. X.; Zouboulis, A. I.; Karapantsios, T. D.; Matis, K. A. *Colloid. Surf. A* **2004**, *242*, 93.
34. Dang, V. B. H.; Doan, H. D.; Dang-Vu, T.; Lohi, A. *Bioresource Technol.* **2009**, *100*, 211.
35. Aravindhan, R.; Fathima, N. N.; Rao, J. R.; Nair, B. U. *Colloid. Surf. A* **2007**, *299*, 232.
36. Duran, C.; Ozdes, D.; Gundogdu, A.; Senturk, H. B. *J. Chem. Eng. Data* **2011**, *56*, 2136.
37. Hameed, B. H.; Tan, I. A. W.; Ahmad, A. L. *Chem. Eng. J.* **2008**, *144*, 235.